Synthesis of Inorganic/Organic Host−Guest Hybrid Materials by Cationic Vinyl Polymerization within Y Zeolites and MCM-41

Stefan Spange,*,† Annett Gräser,† Hardy Müller,† Yvonne Zimmermann,† Petra Rehak,‡ Christian Jäger,‡ Hartmut Fuess,§ and Carsten Baehtz§

Polymer Chemistry, Department of Chemistry, Faculty of Sciences, Chemnitz University of Technology, 09107 Chemnitz, Germany, Institute of Physics, Friedrich-Schiller-University Jena, Max-Wien-Platz 1, D 07743 Jena, Germany, and Materials Science, University of Technology Darmstadt, Petersenstrasse 23, 64287 Darmstadt, Germany

Received February 5, 2001. Revised Manuscript Received August 9, 2001

Cationic guest polymerizations of several vinyl monomers inside the pores of HY zeolites and MCM-41 as hosts have been used for the synthesis of novel organic/inorganic hybrid materials. Substituted vinyl ethers [ROCH=CH_2; R = $-CH_2CH(CH_3)_2$, $-C_2H_5$, $-C_2H_4Cl$, $-C_6H_{11}$], 2,3-dihydrofuran, and *N*-vinylcarbazole can serve this purpose, because their polymerization can be initiated by the active protons in HY zeolite or by coadsorbed arylmethylium ions in MCM-41. The synthesis of well-defined poly(vinyl ethers) or poly(vinylcarbazole) under the conditions of constricted geometry can be achieved by means of cationic host−guest polymerization of the corresponding monomers in MCM-41 (pore diameter 3.6 nm) with $(4\text{-}CH_3OC_6H_4)_2CHCl$ (MeO) or $(C_6H_5)_3CCl$ (TC) as the internal surface initiator. The reaction products are novel polymer/MCM-41 host−guest hybrid materials. The molecular mass of the (enclosed) polymer and the percentage of polymer within the pores of MCM-41 as well as HY zeolite can be adjusted within certain limits. Polymeric products are analyzed by solid-state magic angle spinning cross-polarization $^{13}C\{^1H\}$ NMR spectroscopy and gel permeation chromatography analyses of the obtained polymer fraction after dissolution of the hybrid material in an aqueous potassium hydroxide solution. The formation of conjugated sequences of poly(vinyl ether) segments inside the HY zeolites is caused by successive ether cleavage along the encapsulated polymer chains.

Introduction

The development of inorganic oxide/organic synthetic polymer hybrid materials has been intensively studied during the past decade.[1−28] In this paper we will address the problem of producing flexible polymer chains directly in channels of mesoporous and nanoporous inorganic oxide materials. For this purpose, the inorganic component has been mainly used in powder form (particle agglomerates and zeolite crystals).

To introduce a flexible polymer directly into an ordered mesoporous host material (Y zeolite, MCM-41, or others), two main approaches have been applied thus far (see Chart 1).

The first path of preparation is conceptually very simple. A mobile flexible polymer is threaded through or into the pores of the porous material. The threading

* To whom correspondence should be addressed.
† Chemnitz University of Technology.
‡ Friedrich-Schiller-University Jena.
§ University of Technology Darmstadt.

(1) Mark, J. E.; Lee, C. Y.-C.; Bianconi, P. A. *Hybrid Inorganic−Organic Composites*; American Chemical Society: Washington, DC, 1995; Vol. 585.
(2) Beecroft, L. L.; Ober, C. K. *Chem. Mater.* **1997**, *9*, 1302.
(3) Frisch, H. L.; Mark, J. E. *Chem. Mater.* **1996**, *8*, 1735.
(4) Wen, J.; Wilkes, G. L. *Chem. Mater.* **1996**, *8*, 1667.
(5) Shi, J.; Seliskar, J. C. *Chem. Mater.* **1997**, *9*, 821.
(6) Frisch, H. L.; West, J. M.; Göltner, C. G.; Attard, G. S. *J. Appl. Polym. Sci.* **1996**, *34*, 1823.
(7) Ikeda, Y.; Kohjiya, S. *Polymer* **1997**, *17*, 4417.
(8) Tamaki, R.; Naka, K.; Chujo, Y. *Polym. Bull.* **1997**, *39*, 303.
(9) Tamaki, R.; Horiguchi, T.; Chujo, Y. *Bull. Chem. Soc. Jpn.* **1998**, *71*, 2749.
(10) Crivello, J. V.; Mao, Z. *Chem. Mater.* **1997**, *9*, 1554.
(11) Crivello, J. V.; Mao, Z. *Chem. Mater.* **1997**, *9*, 1562.
(12) Mann, S.; Burkett, S. L.; Davis, S. A.; Fowler, C. E.; Mendelson, N. H.; Sims, S. D.; Walsh, D.; Whilton, N. T. *Chem. Mater.* **1997**, *9*, 2300.
(13) Tamaki, R.; Chujo, Y. *Chem. Mater.* **1999**, *11*, 1719.
(14) Carrado, K. A.; Xu, L. *Chem. Mater.* **1998**, *10*, 1440.
(15) Frisch, H. L.; Xue, Y. *J. Polym. Sci., A: Polym. Chem.* **1995**, *33*, 1979.
(16) Laible, R.; Hamann, K. *Adv. Colloid Interface Sci.* **1980**, *13*, 65.
(17) Tsubokawa, N. *Prog. Polym. Sci.* **1992**, *17*, 417.
(18) Zaper, A. M.; Koenig, J. L. *Polym. Compos.* **1985**, *6*, 156.
(19) (a) Arkles, B. *Chemtech* **1977**, *7*, 766. (b) An excellent review for silicon compounds, their chemistry, and applicability for surface modification is given in: Arkles, B. *Gelest* **2000**, *16*, and references in this catalogue.
(20) Ikeda, Y.; Kohjiya, S. *Polymer* **1997**, *17*, 4417.
(21) Johnson, S. A.; Brigham, E. S.; Ollivier, P. J.; Mallouk, T. E. *Chem. Mater.* **1997**, *9*, 2448.
(22) O'Haver, J. H.; Harwell, J. H.; Evans, L. R.; Waddell, W. H. *J. Appl. Polym. Sci.* **1996**, *59*, 1427 and references therein.
(23) Ou, Y. C.; Yu, Z. Z.; Vidal, A.; Donnet, J. B. *J. Appl. Polym. Sci.* **1996**, *59*, 1321 and references therein.
(24) Vidal, A.; Guyot, A.; Kennedy, J. P. *Polym. Bull.* **1980**, *2*, 315.
(25) Tajima, K.; Aida, T. *Chem. Commun.* **2000**, 2399.
(26) Kageyama, K.; Tamatawa, J.; Aida, T. *Science* **1999**, *185*, 2113.
(27) Johnson, S. A.; Grigham, E. S.; Ollivier, P. J.; Mallouk, T. E. *Chem. Mater.* **1997**, *9*, 2448.
(28) Müller, H.; Rehak, P.; Jäger, C.; Hartmann, J.; Meyer, N.; Spange, S. *Adv. Mater.* **2000**, *22*, 1671.

10.1021/cm011028s CCC: $20.00
Published on Web 09/27/2001

Chart 1. Syntheses of One-Dimensional Polymer/Inorganic Oxide Hybrids

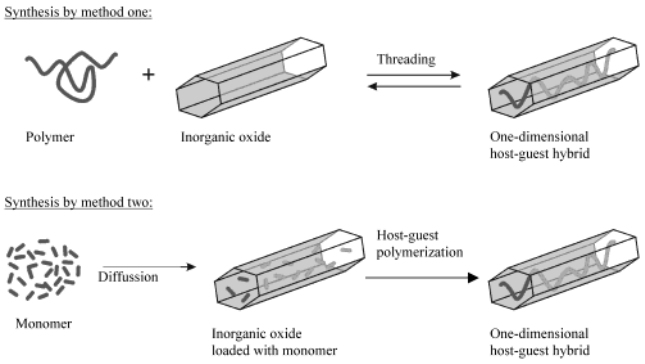

of linear flexible chains into the highly ordered pore systems of HY zeolites or MCM-41 is experimentally very difficult, probably because of the associated loss of entropy.

A further option involves synthesizing the polymer directly in the pore system of a mesoporous silicate or other host (method 2). Various methods have been developed for host−guest polymerization. In pioneering work Bein[29−35] has successfully studied the electropolymerization of pyrrole in HY zeolites and the radical polymerization of methacrylates in MCM-41. In these processes the initiation of the polymerization occurs by chance, on or within the solid material. If the initiator is immobilized by covalent bonding to the inner surface of a mesoporous silicate and/or aluminosilicate (a method used successfully with transition-metal complexes for ethylene polymerization), polyethylene fibers can be synthesized directly inside the mesopores of, e.g., MCM-41.[36−40] A general feature of all host−guest polymerizations is the inner surface chemistry of the host. It should interfere as little as possible, if at all, with the mechanism of the polymerization reaction, for example, by inducing transfer and degradation reactions. In the cationic polymerization of vinyl ethers (VEs) in nanopores of moderately acidic HY zeolites, acid-induced reactions of poly(vinyl ether) (PVE) in the pore system of the zeolite occur. These cause ether cleavage, and conjugated polymer sequences are formed.[41] A brief literature review of host−guest polymerizations in one-dimensional directed inorganic materials is given in Table 1.[42] Tajima and Aida[25] review controlled polymerization with constrained geometries.

Table 1. Examples of Guest Polymerizations of Organic Monomers in One-Dimensional Inorganic Host Materials (for a Review, See Also Ref 25)

guest monomer	inorganic host	catalysis	references
acrylonitrile	MCM-41	radical	30
aniline	Y zeolite	redox	31
pyrrole	Y zeolite	redox	32
pyrrole	Cu mordenite	redox	36
thiophene	Cu mordenite	redox	36
styrene	13X zeolite	radical	3
ethyl acrylate	13X zeolite	radical	6
methyl methacrylate	MCM-41	radical	38
methyl methacrylate	MCM-41	radical	33
methyl methacrylate	Y zeolite, zeolite β	radical	35
methyl methacrylate	ZSM-5, MCM 48	radical	
vinyl ether	HY zeolite	cationic	41
ethylene	MCM-41	metallocene	39
ethylene	MCM-41	metallocene	26
ethylene	MCM-41	metallocene	40
vinyl ether	MCM-41	cationic	42, 43, 44
N-vinylcarbazole	MCM-41	cationic	43, 44

Summarizing the mechanistic aspects of Table 1 leads to the following conclusions. For HY zeolites, mainly direct cationic, radical, and redox polymerizations have been used, because immobilization of surface initiators on HY zeolites affords no advantage. The direct linking of polymers on the internal surface of MCM-41 is possible by using immobilized transition-metal complex initiators. Also, the polymerization of freely mobile vinyl monomers by radical polymerization within MCM-41 has been done. Because of the acidic nature of the inorganic materials considered, anionic polymerizations have not been applied.

In this contribution we consider the application of cationic polymerization of vinyl monomers in Y zeolite (H form) and MCM-41 as inorganic materials.

Cationic polymerization as a method for surface functionalization has been applied to supports such as silica,[44,46] carbon black,[17] and aluminosilicates (montmorillonite clay).[47] The cationic polymerization of suitable vinyl monomers or heterocycles (spiroortho esters) can be initiated either by active protons derived from acidic surface groups or by immobilized cationic-active surface initiators.[17,24] A detailed review of cationic surface polymerizations of organic monomers on inorganic materials is given elsewhere.[46]

Proton (H^+) surface initiation has been observed for aluminosilicates and for protic acids adsorbed on silica.[17,47] Pure silicate materials are usually unable to initiate directly the cationic surface polymerization of VEs, *N*-vinylcarbazole (NVC), styrene, or other vinyl monomers, even in the suspension of solvents which are established for cationic polymerization, e.g., dichloromethane, toluene, or hexane.

Suitable initiators for cationic surface polymerization are halogenoarylmethanes ($R^1R^2R^3CX$; X ≙ Cl or Br) which become cationically active on acidic surfaces.[48−52]

(29) Wu, C.-G.; Bein, T. *Science* **1994**, *264*, 1757.
(30) Wu, C.-G.; Bein, T. *Chem. Mater.* **1994**, *6*, 1109.
(31) Bein, T.; Enzel, P. *Angew. Chem.* **1989**, *101*, 1737.
(32) Enzel, P.; Bein, T. *J. Phys. Chem.* **1989**, *93*, 6270.
(33) Moller, K.; Bein, T.; Fischer, R. X. *Chem. Mater.* **1998**, *10*, 1841.
(34) Meinershagen, J. L.; Bein, T. *J. Am. Chem. Soc.* **1999**, *121*, 448.
(35) Moller, K.; Bein, T. *Chem. Mater.* **1998**, *10*, 2950.
(36) Millar, G. J.; McCamm, G. F.; Hobbis, C. M.; Bowmaker, G. A.; Conney, R. P. *J. Chem. Soc., Faraday Trans.* **1994**, *90*, 2579.
(37) Matsumoto, A.; Kitajima, T.; Tsutsumi, K. *Langmuir* **1999**, *15*, 7626.
(38) Ng, S. M.; Ogino, S.; Aida, T.; Koyano, K. A.; Tatsumi, T. *Macromol. Rapid Commun.* **1997**, *18*, 991.
(39) Lehmus, P.; Rieger, B. *Science* **1999**, *285*, 2081.
(40) Weckhuysen, M.; Ramachandra Rao, R.; Pelgrims, J.; Schooheydt, R. A.; Bodart P.; Debras, G.; Collart, O.; Van Der Voon, P.; Vausani, E. F. *Chem. Eur. J.* **2000**, *6*, 2960.
(41) Gräser, A.; Spange, S. *Chem. Mater.* **1998**, *10*, 1814.
(42) Spange, S.; Gräser, A.; Rehak, P.; Jäger, C.; Schulze, M. *Macromol. Chem. Rapid Commun.* **2000**, *21*, 150.
(43) Spange, S.; Zimmermann, Y.; Gräser, A. *Chem. Mater.* **1999**, *11*, 3245.
(44) Spange, S.; Gräser, A.; Huwe, A.; Kremer, F.; Tintemann, C.; Behrens, P. *Chem. Eur. J.* **2001**, *7*, 3722.
(45) (a) Spange, S.; Höhne, S.; Francke, V.; Günther, H. *Macromol. Chem. Phys.* **1999**, *200*, 1655. (b) Spange, S.; Langhammer, E. *Macromol. Chem. Phys.* **1997**, *198*, 2993.
(46) (a) Spange, S. *Prog. Polym. Sci.* (Review) **2000**, *25*, 781. (b) Spange, S.; Eismann, U.; Höhne, S.; Langhammer, E. *Macromol. Symp.* **1997**, *126*, 223.
(47) (a) Biswas, M.; Ray, S. S. *Polymer* **1998**, *39*, 6423. (b) Ray, S. S.; Biswas, M. *Mater. Res. Bull.* **1999**, *34*, 1187.

Chart 2. Possible Location of Several Vinyl Monomers (Left) and (4-$CH_3OC_6H_4)_2CHCl$ and $(C_6H_5)_3CCl$ (Right) in a MCM-41 Gate

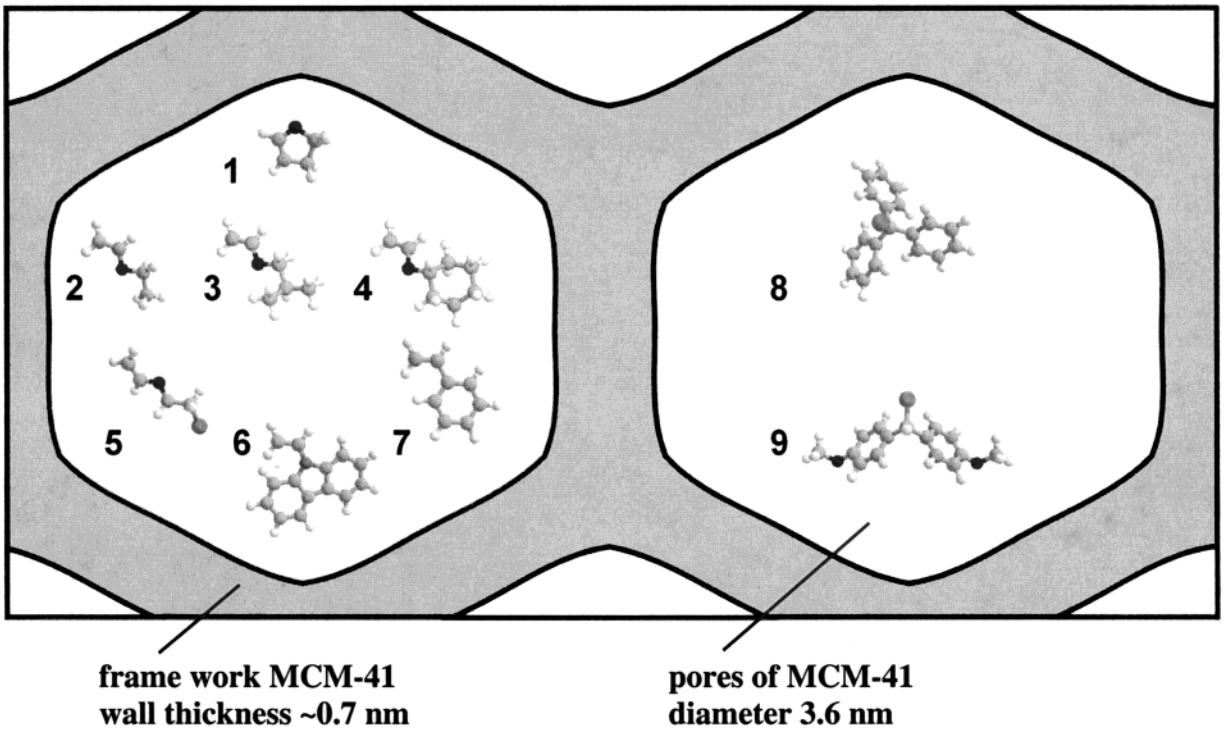

On the basis of our own knowledge and experience of the mechanism of cationic surface polymerization, we have defined reaction conditions enabling preferential polymerization in the silicate channels.[44] Equation 1 gives an expression for the rate of total monomer consumption, taking into consideration the reaction steps of the cationic propagation reactions in the channels (host−guest, HG), those on the outer surface of the MCM-41 (OS), and those in the surrounding solution (S). If there is exclusive cationic host−guest polymerization, terms 2 and 3 in eq 1 vanish.

$$-\mathrm{d}[\mathrm{M}]/\mathrm{d}t = \underset{1}{k_{\mathrm{pHG}}[\mathrm{R}^+]_{\mathrm{HG}}[\mathrm{M}]_{\mathrm{HG}}} + \underset{2}{k_{\mathrm{pOS}}[\mathrm{R}^+]_{\mathrm{OS}}[\mathrm{M}]_{\mathrm{OS}}} + \underset{3}{k_{\mathrm{pS}}[\mathrm{R}^+]_{\mathrm{S}}[\mathrm{M}]_{\mathrm{S}}} \quad (1)$$

This can be achieved best experimentally by keeping the concentration of the carbenium ion in the surrounding solution, $[R^+]_S$, or on the outer surface, $[R^+]_{OS}$, as small as possible. Arylmethyl halides ($XCR^1R^2R^3$) are used as cationically inactive initiators for this host−guest polymerization. They are essentially inactive in solution but are activated specifically on the inner surface of, for example, porous siliceous materials.[42,44] For cationic VE polymerization on silica,[48] chlorotriphenylmethane (TCl) and chlorobis(4-methoxyphenyl)-methane (MeO) (Table 2 and Chart 2) have been selected as suitable cationically active surface initiators. Both compounds have specific advantages as surface initiators on silica for cationic polymerization. Both cations have approximately the same electrophilicities as those expressed by their pK_{R+} values[53,54] and similar size. They also fit into the channel of MCM-41 as shown in Chart 2.

Table 2. Physical Properties and Sources of the Porous Inorganic Host Materials Used

porous material	BET surface (measd) [m^2/g]	average pore radius [nm]	supplier
HY zeolite	715	0.37	Degussa AG
HY zeolite [Wessalith DAY-P]	618	0.37	Degussa AG
MCM-41	754	1.82	Mobil Oil

Other carbenium precursors which involve strong electrophilic carbenium ions such as $(C_6H_5)_2CHCl$ and $(4\text{-}CH_3C_6H_4)_2CHCl$ are very weakly cationically active on MCM-41.[55] With silica as the catalyst, the largest apparent rate constant k' (maximum point of the curve log k' versus pK_{R+}) for the hydride transfer reaction of 1,4-cyclohexadiene with carbenium ions has been found for MeO with $pK_{R+} = -5.6$.[46a,51]

The objective of this work is a systematic study of the influence of both the monomer structure and concentration on the composition and structural properties of

(48) Eismann, U.; Spange, S. *Macromolecules* **1997**, *30*, 3439.
(49) Spange, S. *Polym. Sci.* **1993**, *35* (11), 1581; *Vysokomol. Soedin., Ser. A & B* **1993**, *35*, 1873.
(50) Adolph, S.; Spange, S.; Zimmermann, Y. *J. Phys. Chem. B* **2000**, *104*, 6417.
(51) Spange, S.; Adolph, S.; Walther, R.; Zimmermann, Y. *J. Phys. Chem.* **2001**, submitted for publication.
(52) Spange, S.; Fährmann, A.; Reuter, A.; Walther, R.; Zimmermann, Y. *J. Phys. Org. Chem.* **2001**, *14*, 271.
(53) (a) Mayr, H.; Patz, M. *Angew. Chem.* **1994**, *106*, 990; *Angew. Chem., Int. Ed. Engl.* **1994**, *33*, 938. (b) Mayr, H. Ionic Polymerization and Related Processes. In *Rate Constants and Reactivity Ratios in Carbocationic Polymerizations*; Puskas, J. E., et al., Eds.; Kluwer Academic Publishers: Dordrecht, The Netherlands, 1999; p 99.
(54) (a) Deno, N. C.; Schriesheim, J. A. *J. Am. Chem. Soc.* **1955**, *77*, 3051. (b) Deno, N. C.; Jaruzelski, J. J.; Schriesheim, J. A. *J. Am. Chem. Soc.* **1977**, *77*, 3051. (c) Jaruzelski, J. J.; Schriesheim, J. A. *J. Org. Chem.* **1954**, *19*, 155.
(55) Zimmermann, Y.; Spange, S., unpublished results.

Table 3. Largest Dimension of the Monomers and Initiator Molecules Used in This Work

guest molecule			size [nm][a]
2,3-dihydrofuran	DHF	1	0.47
ethyl vinyl ether	EVE	2	0.65
isobutyl vinyl ether	IBVE	3	0.78
cyclohexyl vinyl ether	CHVE	4	0.76 (equatorial)/ 0.80 (axial)
2-chlorethyl vinyl ether	ClEVE	5	0.70
N-vinylcarbazole	NVC	6	0.90
2-methoxypropene	MP		0.53
styrene		7	0.78
chlorotriphenylmethane[b]	TCl	8	0.93 (0.91)
chlorobis(4-methoxy-phenyl)methane	MeO	9	1.34

[a] Numbers refer to the positions in Chart 3. [b] In catalogues of chemicals, chlorotriphenylmethane often is denoted as triphenylmethyl chloride. However, this suggests an ionic compound (salt), which is not correct.

host−guest nanocomposite materials. For this purpose, cationic host−guest polymerizations of substituted VEs and NVC have been used.

Table 2 contains the monomers and initiators used in this study, their abbreviations, and optimum sizes calculated with molecular modeling.

Experimental Section

Materials. For the experiments we have chosen HY zeolite and a siliceous MCM-41. The physical and chemical properties of the materials are given in Table 3.

To achieve complete desorption of reversibly bound water from the nanoporous materials, they were baked out in a muffle oven at a rate of 1 K/min from room temperature to 400 °C and maintained there for at least 12 h. The hot samples were transferred to Schlenk tubes under argon and then cooled. Generally they were used immediately after cooling.

The solvents ethanol, hexane, carbon tetrachloride, toluene, and dichloromethane and the monomers EVE, IBVE, CHVE, ClEVE (99%, Aldrich), MP, styrene, and DHF were dried over calcium hydride. (See Table 3 for description of acronyms.) All chemicals were distilled before use. NVC was recrystallized from hexane.

General Procedure for the Polymerization of VEs on Supports. Host materials (ca. 100−200 mg) were placed in dichloromethane (10−20 mL) to preclude water adsorption on MCM-41 or HY zeolite. The Schlenk tube was then thermostated for 10 min, and the arylmethyl initiator was added (typical quantities: $m_{MeO} = 100$ mg; $n_{MeO} = 37$ mmol for MCM-41). After the addition of 0.10−2.0 mL of monomer under stirring, the host material decolorized, because the carbenium ion reacts with the monomer, although not always completely. The polymerizations were carried out at −25 °C, unless otherwise stated. The reaction was finished after 24 h. The host materials were then separated from the solvent and from the soluble extractable polymer by suction filtration on a G4 glass frit and washed three times with 15 mL of dichloromethane. The combined solvent fractions were washed with 20 mL of an aqueous 5% sodium hydrogen carbonate solution to remove acid and dried with sodium sulfate. In the cases of PEVE, PIBVE, and PClEVE, dichloromethane was removed on a rotary evaporator and the remaining polymer was dried under vacuum. The solutions of the polymers PCHVE, PDHF, PSt, and PNVC were concentrated to ca. 10 mL and the polymers precipitated in 150 mL of ice-cold methanol, collected by suction filtration, and dried in vacuo.

PEVE and PIBVE polymers were viscous to highly viscous (depending on the molecular mass), sticky, and colorless. PClEVE was viscous and yellow to brown. PCHVE, PDHF, PSt, and PNVC were white powders.

The siliceous part of the MCM-41/polymer hybrid is readily soluble in aqueous potassium hydroxide. The hybrid (ca. 100 mg) was suspended in 30 mL of 5% potassium hydroxide and covered with 30 mL of hexane. This mixture was shaken for about 30 min until the hybrid was completely dissolved. The polymer previously enclosed in the hybrid thus passes into the organic phase. After phase separation, the aqueous phase was extracted twice with 10 mL portions of hexane. The combined organic phases were dried with sodium sulfate and filtered. Residual solvent is completely removed in vacuo. PVEs are resistant to the aqueous potassium hydroxide solution used. The extractable polymer fraction was treated with the solution and worked up as described above. The molecular mass distributions were identical before and after the analogous treatment of the polymer.

Functionalization Reaction of MCM-41 with $(C_2H_5O)_2CHCH_3$. A total of 0.182 g of MCM-41 (dried at 400 °C) was suspended in 10 mL of tetrachloromethane and an excess of 2 mL of acetaldehyde diethyl acetal (AAD) added. The previously transparent suspension of MCM-41 in CCl_4 becomes turbid after the addition of AAD. The mixture was refluxed for 70 min, filtered, carefully washed, and dried in vacuo.

The functionalized MCM-41 contains 3.85 wt % carbon determined by quantitative elemental analysis.

UV/Vis Spectroscopic Measurements. The UV/vis absorption maxima of the triphenylmethyl compounds adsorbed on the solid acid catalyst were recorded using a diode array UV/vis spectrometer (Carl Zeiss MCS 4) with glass fiber optics. The concentration of the triphenylmethyl compound was about 1−10 mg/g of catalyst. The transparent support/1,2-dichloroethane suspensions were measured as previously reported.[43] This yields good-quality transmission spectra with excellent reproducibility (less than $\lambda_{max} \pm 1$ nm).

Surface titrations of MCM-41 with chloroarylmethane derivatives were carried out directly in the slurry. The stock solution of chloroarylmethane was added by a glass syringe through a silicone septum. The spectra were recorded immediately after the addition with an immersion cell (TSM 5) which is placed directly in the slurry.

Brunauer−Emmett−Teller (BET) Measurements. The BET surface area was measured with sorption of N_2 at 77 K using a Sorptomatik 1900 (Fisons). For the measurements, the PVE/HY zeolite hybrid materials were dried at 110 °C. For the polymer/MCM-41 hybrid materials, a drying temperature of 80 °C under vacuo was used.

Solid-State NMR Spectroscopy. The cross-polarization magic angle spinning (CP-MAS) (28 kHz) ^{1}H and (4 kHz) ^{13}C-{^{1}H} NMR spectra were recorded on a Bruker AMX 400, and the MAS (6 kHz) ^{29}Si NMR spectra were recorded on a Tecmag spectrometer. Chemical shifts were determined by reference to standard substances (i.e., adamantane for the ^{13}C signals). Recycle delays were 2−4 K.

X-ray Diffraction (XRD) Measurements. The powder diffractograms were measured using STOE-STADI-P with Debye−Scherrer geometry. The patterns were recorded with Cu Kα_1 radiation with a wavelength of $\lambda = 0.154\,056$ nm from a Ge monochromator. The step width employed was 0.02° (in 2θ).

Gel Permeation Chromatography (GPC) Analyses. The molecular weight distributions (MWD) of the soluble polymers were determined by GPC using a Knauer GPC. Three Euro Gel columns with 100, 1000, and 10 000 Å pore sizes were used. Measurements were carried out at 25 °C using THF as the eluent and polystyrene calibration. Quantitative determination of polymer fractions occurred with refraction and viscosity detection.

Scanning Electron Microscopy. The morphological structure of the hybrid materials was characterized by transmission electron microscopy (Zeiss EM 912 Omega) at an accelerating voltage of 120 kV. The hybrid specimens were prepared by embedding the hybrid powder in epoxy resin and ultramicrotoming (Leica Ultracut UCT).

Quantitative Elemental Analysis. The amounts of carbon of the solid hybrid materials were determined by quantitative

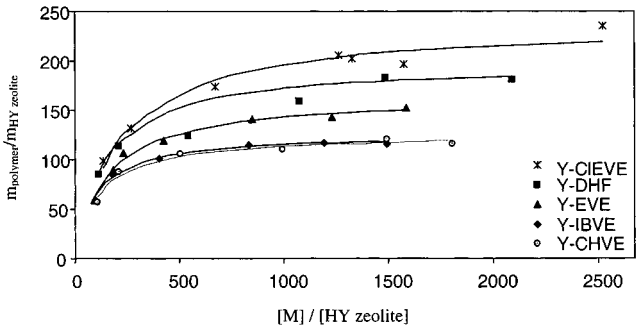

Figure 1. Ratio of polymer generated within the HY zeolite [$m_{polymer}/m_{HY\ zeolite}$] as a function of the initial monomer/HY zeolite ratio ([M]/[HY zeolite]).

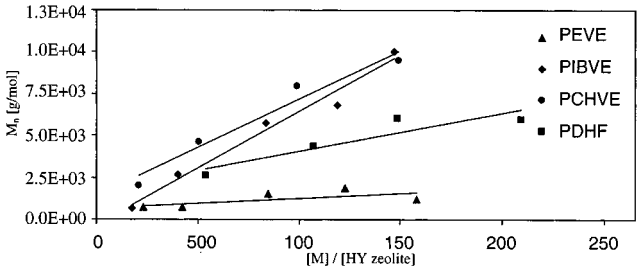

Figure 2. Average molecular weight (M_n) of the soluble polymer fraction obtained by HY zeolite initiation as a function of the initial monomer/HY zeolite ratio.

elemental analysis. The analyses were done with an analysator Vario EL from Elementar GmbH.

Results and Discussion

Cationic Host−Guest Polymerization of Substituted VEs in HY Zeolites. Several $R^1R^2R^3CCl$ compounds adsorb fairly well on inorganic oxides.[56,57] However, on HY zeolites only the external surface of the material is of relevance because $R^1R^2R^3CCl$ is too large to enter.[57b] Therefore, initiation of cationic polymerization of VEs within HY zeolites is achieved only with the mobile protons of the HY zeolite. For this purpose, several Na/H-exchanged Y zeolites have been checked.[41] For these experiments, an Na/H-exchanged material with about 80% H form has been found to be suitable.[41]

A systematic extension to this study shows that the polymer content can be precisely controlled by the monomer/HY zeolite ratio (see Figure 1). Also, the molecular weight of the soluble polymer fraction can be controlled by the same parameter, as shown in Figure 2.

However, the soluble fraction is only of indirect importance for the interpretation of the results of host−guest polymerization, because it is formed at external surface sites of the HY zeolite. The soluble PVE fractions are white (colorless) polymer melts. Structural data are in agreement with the literature. Because the monomer is of a relatively large size, it cannot penetrate rapidly into the HY zeolite pores, and initiation takes place on the external surface. This is shown by the linear plots and significantly larger slope of M_n as a function of [monomer]/[HY zeolite] for cyclohexyl vinyl ether and isobutyl vinyl ether, whereas for the small-sized ethyl vinyl ether, the slope is negligible (Figure 2). This is caused by the presence of EVE and DHF on the internal surface of the HY zeolite.

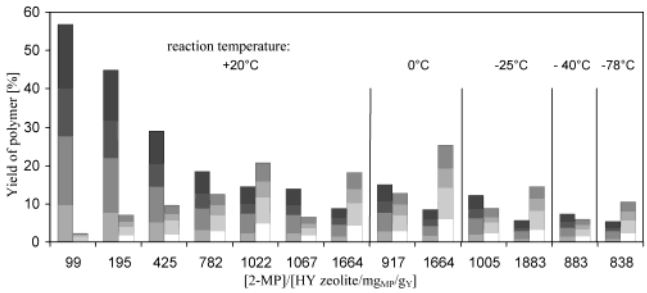

Figure 3. Yield of oligo(2-MP) within the HY zeolite (■) and of the soluble fraction (□) as a function of the [2-MP]/[HY zeolite] ratio and reaction temperature.

Within this work the polymer fraction remaining in the pores of the HY zeolite after polymerization is of interest. The influence of the monomer/HY zeolite ratio on the mass ratio of polymer generated on zeolite and in the soluble fraction is shown for the cationic host−guest polymerization of 2-methoxypropene (2-MP) in the HY zeolite host (Figure 3).

This 2-MP monomer shows outstanding polymerization behavior on HY zeolites. Usually, 2-MP does not polymerize well in a homogeneous solution using standard conditions for cationic polymerization, for steric and electronic reasons.[58] When 2-MP is loaded on the HY zeolites, it produces oligomeric products of adjustable molecular weight.[59]

The optimized mass balance of PVE generated inside the HY zeolite has been determined for all VE monomers studied. The results are shown in Table 4, which also contains literature results for toluene adsorption and methyl methacrylate polymerization inside the HY zeolite for comparison.[33] The loading PVE/HY zeolite increases as the size of the VE monomer decreases. This is an expected and reasonable result. The largest amount of loading has been found for 2-chloroethyl vinyl ether. This monomer does not rapidly form polymers "either outside" or inside the HY zeolite, because it possesses the lowest reactivity for cationic polymerization of all monomers (see the results for MCM-41 host−guest polymerization below) used in this work.[60] Therefore, the monomer can deeply penetrate into the channel. The comparison with the results from the literature in Table 4 shows good agreement with our results.

The PVE fractions that remain in the HY zeolite are colored. The color of the encapsulated PVE polymer in the HY zeolite is attributed to conjugated sequences that are formed by acid-induced ether cleavage of the polymer by the active protons in HY (see Chart 3).[41]

This mechanism has been established using gas chromatography (GC) analyses of soluble decomposition products, UV/vis, and solid-state NMR spectroscopy of the PVE/HY zeolite hybrid materials.[41] Acetaldehyde has not been found as the decomposition product, which is expected because the VE monomer would be cleaved

(56) Leftin, H. P., Olah, G. A., Schleyer, P. v. R., Eds. *Carbonium Ions*; Wiley: New York, 1968; Vol. 1, p 363.

(57) (a) Corma, A. *Chem. Rev.* **1995**, *95*, 559. (b) Cano, M. L.; Corma, A.; Fornes, V.; Garcia, H.; Miranda, M. A.; Baerlocher, C.; Lengauer, C. *J. Am. Chem. Soc.* **1996**, *118*, 11006.

(58) Nuyken, O.; Kröner, H. *Macromol. Chem.* **1990**, *191*, 1.

(59) Gräser, A.; Spange, S. *Polym. Bull.* **2001**, in preperation. The molecular mass of the soluble oligo(2-methoxypropene) fraction is strongly dependent on the reaction temperature used. In increasing the temperature from −78 to +20 °C, M_n decreases from 6000 to 1000 g mol^{-1}.

(60) Gotta, M. F.; Mayr, H. *J. Org. Chem.* **1998**, *63*, 9769.

Table 4. Largest Possible Amount of Consumed Monomer per Gram of HY Zeolite Using the Optimum Monomer/HY Zeolite Ratio

batch	$m_{monomer}/m_{HY}$ [mg_M/g_Y]	$m_{polymer}/m_{HY}$ [mg_P/g_Y]	$n_{polymer}/m_{HY}$ [$mmol_P/g_Y$][a]
Y-DHF-6	2091	181.0	2.58
Y-ClEVE-7	2522	234.0	2.20
Y-EVE-7	1583	152.1	2.11
Y-MP-7	1664	146.6	2.03
Y-IBVE-6	1496	116.2	1.16
Y-CHVE-6	1803	116.1	0.92
comparison			
toluene/HY[b]		$m_{toluene}/m_{HY} = 150$	$n_{toluene}/m_{HY} = 1.63$
PMMA/NaY[c]		$m_{PMMA}/m_{NaY} = 300$	$n_{PMMA}/m_{NaY} = 2.99$

[a] $n_{polymer}$ denotes the total amount of consumed monomer. [b] Supplier data: the toluene content within the HY zeolite amounts to 15 g of toluene/100 g of zeolite at $T = 293$ K and $p/p_0 = 0.1$. This corresponds to 1.63 mmol of toluene/g of HY zeolite. [c] According to ref 33.

Chart 3. Proposed Formation of a Trienylium Structure Induced by Acidic Cleavage of a PVE Section within the HY Zeolite

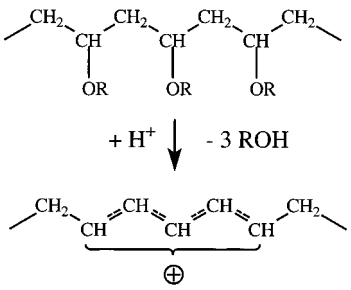

Table 5. Comparison of the UV/Vis Absorption Maxima Observed during the Host−Guest Polymerization of Several VEs within the HY Zeolite and of a Model Compound from the Literature[61]

polyenylic cation[a]	λ_{max} [nm]						
	ref 61	DHF	EVE	IBVE	CHVE	ClEVE	MP
$n = 1$	397	385	377	379	383	380	405
$n = 2$	473	470	465	464	448	466	485
$n = 3$	550	550	554	550		530	560
$n = 4$	625		619			614	
$n = 5$	702		693				

[a] $[(CH_3)_2C{=}CH(CH{=}CH)_nC(CH_3)_2]^+$ in 80% H_2SO_4 from ref 61a.

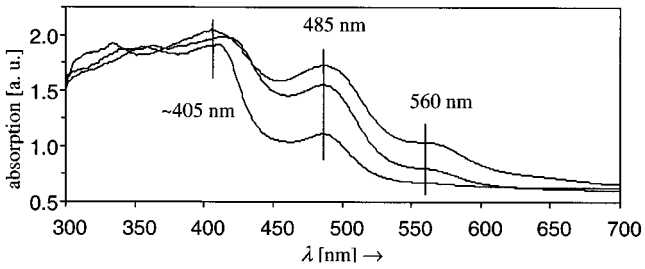

Figure 4. UV/vis spectra measured during the host−guest oligomerization of 2-MP within the HY zeolite as a function of the reaction temperature. From the bottom to the top: 248, 273, and 393 K. Note: At 248 K, no tetraenylium ion is formed.

first. The assignment of UV/vis absorption bands observed during the host−guest polymerization of various VEs to corresponding polyenylic cationic model compounds[61] is compiled in Table 5. Furthermore, Figure 4 shows the influence of the reaction temperature on three characteristic UV/vis spectra recorded during the oligomerization of 2-MP inside the HY zeolite. The higher the reaction temperature, the larger is the extent of conjugation (*n* from Table 5). This also indicates clearly the postreaction of the encapsulated chain by active protons inside the HY zeolite.

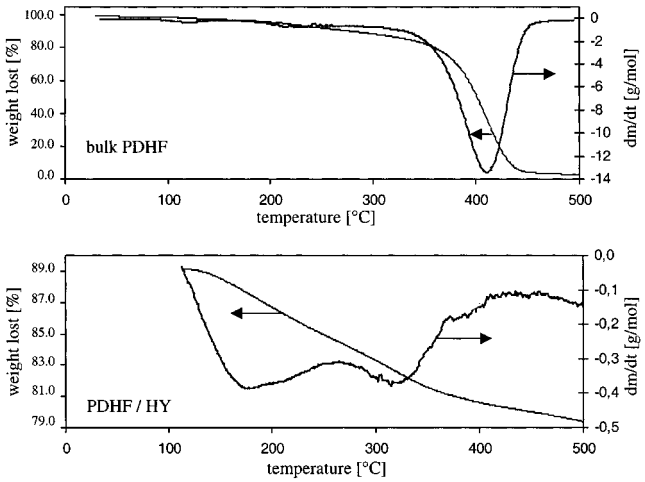

Figure 5. Influence of the HY zeolite host matrix on the thermal decomposition of PDHF compared to bulk PDHF.

As long as water and oxygen are excluded, the PVE/HY zeolite hybrid materials can be stored over a rather long time period (weeks) without losing their optical properties. However, they are thermally less stable than pure bulk PVEs. Figure 5 shows two typical thermogravimetric results for the pure PDHF and the PDHF/HY zeolite hybrid material.

The PDHF fraction within the HY zeolite decomposes at about 200 °C, whereas the PHDF bulk polymer remains stable up to 350 °C. The thermal instability of the PVE phase inside the HY zeolite is caused by elimination initiated by the acidic protons inside the HY zeolite resulting in byproducts (alcohol, ether, and olefins).[41] Thermogravimetric analyses for several PVE/HY zeolite materials batched with and without the presence of oxygen are summarized in Table 6.

One fundamental question remains for all hybrid organic/inorganic materials produced by host−guest polymerization: where is the main fraction of the polymer really located, inside or on the external surface of the resulting hybrid material? After the polymerization is complete, the materials are carefully washed and extracted in order to remove physically bounded polymers from the external surface. BET measurements are expected to provide some idea of the percentage of pore filling. With increasing polymer loading of PVE, the BET surface area of HY zeolite hybrid material strongly

(61) (a) Sorensen, T. S. *J. Am. Chem. Soc.* **1965**, *87*, 5075. (b) Olah, G. A.; Pittmann, C. U., Jr.; Sorensen, T. S. *J. Am. Chem. Soc.* **1966**, *88*, 2331.

Table 6. Results of the Thermogravimetric Investigations of Several PVE/HY Zeolite Hybrid Materials

batch	mg_P/g_Y [%]	weight lost [%] drying[a] (30−110 °C)	decomposition[b] (110−500 °C)	calcination[c] (500−800 °C)
HY zeolite	0.0	26.47		
Y-IBVE-4	11.5	12.68	10.32 (200)[d]	3.95
Y-CHVE-4	11.0	12.07	8.74 (200)[d]	5.85
Y-ClEVE-5	20.2	8.88	13.46 (210)[d]	7.39
Y-EVE-5	14.1	10.79	9.58 (190)[d]	6.82
Y-DHF-4	15.9	10.80	10.19 (190, 320)[d]	10.35
Y-MP-4	14.5	9.60	10.29 (270)[d]	6.21

[a] In a helium flow with a heating rate of 50 K/min and then 30 min of constant heating at $T = 110$ °C. [b] Decomposition of the polymer in helium flow between $T = 110$ and 500 °C. Heating rate: 10 K/min. [c] Calcination of the remaining carbon phase in air between $T = 500$ and 800 °C. Heating rate: 20 K/min and then 15 min of constant burning up at $T = 800$ °C. [d] The number in parentheses denotes the temperature of maximum polymer decomposition.

decreases. However, linear curves are not obtained, and at times the measurements were poorly reproducible because of the different water contents. Therefore, XRD experiments have been carried out for selected samples.

The Bragg reflections of the pure HY zeolite are in agreement with the literature data.[62,63] Their positions are not changed after the zeolite has been used as the host for VE polymerization. However, the intensity ratios of the reflections at $2\theta = 10°$ and 12° as well as those at $2\theta = 18.5°$ and 20.5° are significantly influenced by the amount of polymer inside the HY zeolite. Increasing the amount of polymer results in a decrease of the intensity ratio of the signal at 10°/20° (see Figure 6). Results imply clearly that the amount of polymer inside the pores has changed.[64]

Hence, the XRD measurements support the assumption that the polymers are inside the HY zeolite pores and that the HY skeleton is not decomposed by the guest polymerization. The precise position of the polymer sections in the loaded host cannot be determined by this method.[64]

Cationic Guest Polymerization of VEs and NVC inside an MCM-41 Host. In a previous paper, we reported that the polymerization of VEs and NVC can be initiated within MCM-41 by a very small fraction of active protons.[43] However, the use of additional internal initiators inside MCM-41, like the halogenoarylmethane compounds (Chart 4), significantly improves the initiation reaction and molecular mass control of the polymer generated.[44] As mentioned, a particularly useful initiator for cationic host−guest polymerization is $(4\text{-}CH_3OC_6H_4)_2CHCl$. In contrast to nonporous materials such as Aerosil 300, the adsorption of $(4\text{-}CH_3OC_6H_4)_2CHCl$ and $(C_6H_5)_3CCl$ on MCM-41 takes place slowly.[44,50] Figure 7 shows the UV/vis spectrum after the adsorption of $(4\text{-}CH_3OC_6H_4)_2CHCl$ in MCM-41 in dichloromethane.

Sometimes the chemisorption of $(4\text{-}CH_3OC_6H_4)_2CHCl$ in MCM-41 can yield ambiguous results. Besides the expected UV/vis absorption derived from the carbenium ion at $\lambda = 511$ nm, a second UV/vis absorption band at about $\lambda = 348/385$ nm appears. This new UV/vis absorption band is due to the radical $(4\text{-}CH_3OC_6H_4)_2\text{-}CH^{\bullet}$.[66] However, its concentration is rather low, and VEs do not polymerize by radical initiation. Thus, we presume that this effect has no influence on the host−guest polymerization. The formation of the radical is not observed when MeO is adsorbed on Aerosil.[50] The temperature influence on the adsorption−ionization equilibrium of $(4\text{-}CH_3OC_6H_4)_2CHCl$ on MCM-41 is reversible as shown in Figure 8.

With decreasing temperature, the carbenium ion UV/vis absorption band at $\lambda = 511$ nm increases, indicating an exothermic process for the adsorption−ionization of $(4\text{-}CH_3OC_6H_4)_2CHCl$ on MCM-41.[65]

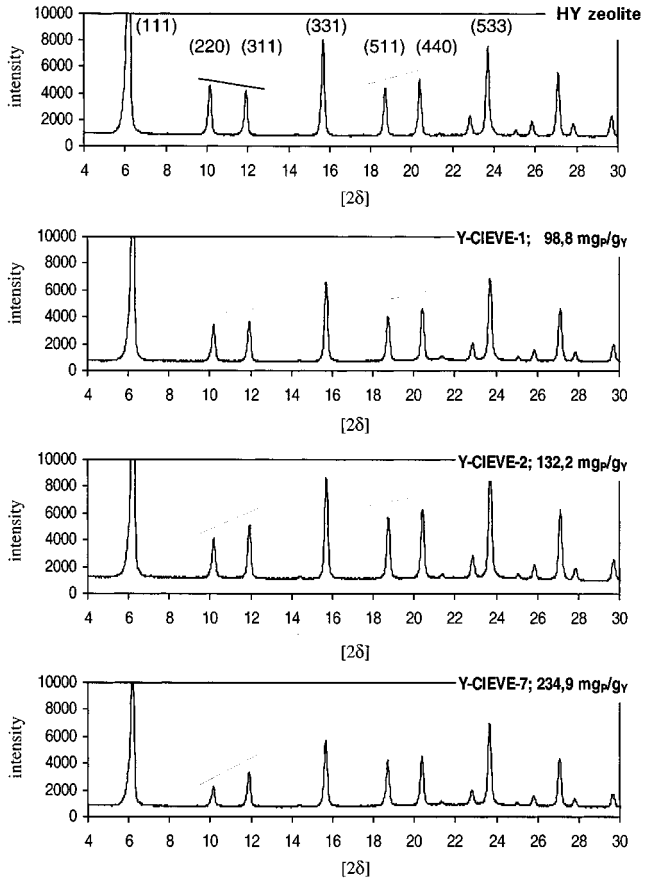

Figure 6. XRD diffraction patterns of the pure HY zeolite (top) and three PClEVE/HY samples, with increasing loading of polymer from the top to the bottom. The lines added stress the change of intensity of the reflections which indicate the loading of the pores.

Chart 4. Cationic Initiation and Propagation of Substituted VE inside MCM-41

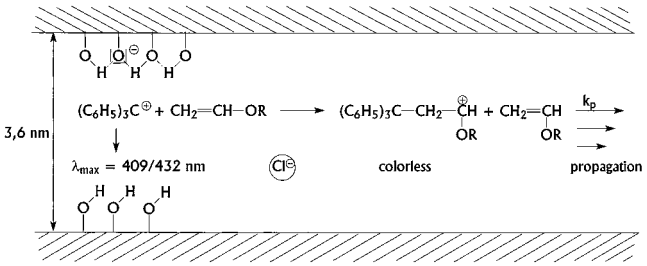

(62) Steinmetz, B.; Zechlin, J.; Przybyla, C.; Tesche, B.; Fink, G. *Nach. Chem. Tech.* **2000**, *48*, 12.

(63) Baur, W. H. *Am. Miner.* **1964**, *49*, 697 (internet: www-iza-sc.csb.yale.edu/IZA-SC).

(64) Baehtz, C.; Ehrenberg, H.; Fuess, H. *Phys. Chem. Chem. Phys.* **2000**, *2*, 5764.

(65) Schneider, S.; Mayr, H.; Plesch, P. H. *Ber. Bunsen-Ges. Phys. Chem.* **1987**, *91*, 1369.

(66) Bartl, J.; Steenken, S.; Mayr, H.; McClelland, R. A. *J. Am. Chem. Soc.* **1990**, *112*, 6918.

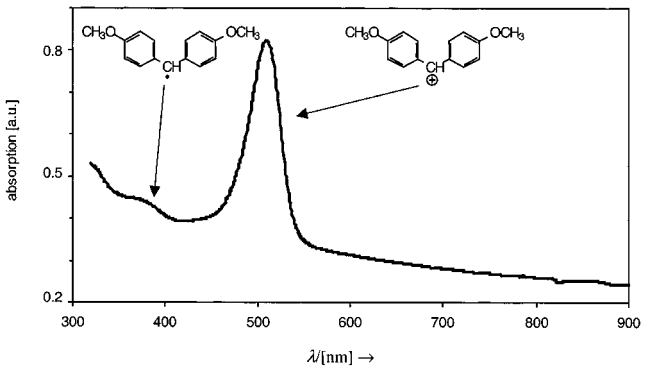

Figure 7. UV/vis spectrum of $(4\text{-}CH_3OC_6H_4)_2CHCl$ adsorbed inside MCM-41 in CH_2Cl_2 at 293 K.

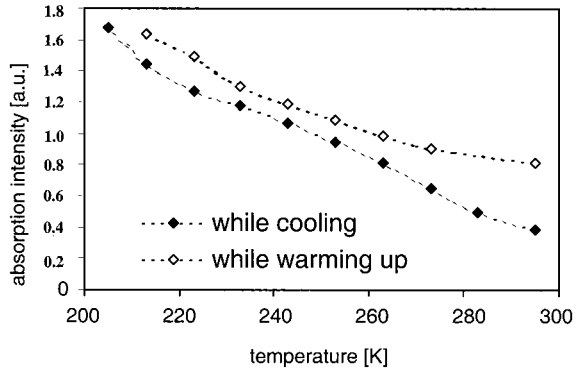

Figure 8. Reversible change of the intensity of the $(4\text{-}CH_3OC_6H_4)_2CH^+$ carbenium UV/vis absorption at $\lambda = 511$ nm inside MCM-41 as a function of temperature in dichloromethane.

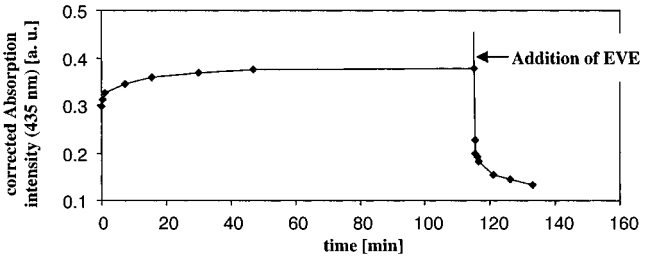

Figure 9. Intensity of the UV/vis absorption of $(C_6H_5)_3C^+$ at $\lambda = 435$ nm as a function of time and after addition of ethyl vinyl ether. Experimental conditions: 15.6 mg (56 μmol) of TCl and 67.2 mg of MCM-41; solvent, 10 mL of dichloromethane; monomer, 200 μL (2.091 mmol; M/I = 37.4) of EVE; temperature, 293 K.

Chart 4 shows the initiation of a VE with triphenylmethylium ion inside MCM-41 and the suggested propagation reaction. For this experiment, $(C_6H_5)_3CCl$ is adsorbed on MCM-41 from a dichloromethane solution. The corresponding UV/vis absorption of $(C_6H_5)_3C^+$ at $\lambda = 410/435$ nm on MCM-41 has been measured by means of the immersion cuvette. Its intensity remains constant after 40 min of adsorption time. After EVE is added, the decrease in the intensity of the UV/vis absorption of $(C_6H_5)_3C^+$ at $\lambda = 410/435$ nm on MCM-41 is easily seen (Figure 9).

The negative charge of the "counterion" keeping the propagating chain in place is located on the internal wall of the MCM-41 skeleton. The proton exchange transfer reaction of the surface silanol groups occurs rapidly.[46b] We presume that the propagation reaction occurs slower than the migration of the internal protons. Conceivably,

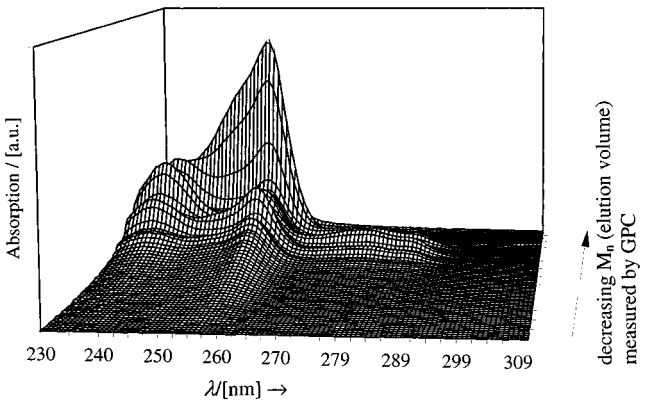

Figure 10. UV/vis spectra of bis[(4-methoxyphenyl)methane] headgroup functionalized PVE fractions depending on the molecular weight separated by GPC analyses using a continuously working UV/vis flow cell as the detector connected via glass fibers with the UV/vis spectrometer.

the rate of propagation k_p versus termination is limited by the intrinsic ratio of both reactions.

The arylmethane headgroup covalently linked to the PVE chain can be seen by UV/vis spectroscopy of the polymer fraction isolated from the inside of the MCM-41. Each molecular weight fraction of the polymer contains a MeO headgroup as shown by the UV/vis band at $\lambda_{max} = 256$ nm in each of the soluble PVE fractions separated by GPC (Figure 10).

Linking of the arylmethane headgroup at the PVE chain has been seen by ^{1}H NMR spectroscopy of the soluble polymer (for details, see refs 48 and 67).

Approximately 300−400 mg of polymer can be generated per 1 g of MCM-41 by this procedure. Typical plots for polymer generated inside MCM-41 as a function of the monomer/initiator ratio are shown in Figure 11a.

Similar curves are obtained when the amount of generated polymer inside MCM-41 is plotted versus the [monomer]/[MCM-41] mass ratio used (Figure 11b).

Despite the absence of internal surface initiators $(4\text{-}CH_3OC_6H_4)_2CH^+$ or $(C_6H_5)_3C^+$ for some experiments (hollow points in Figure 11a), the polymer mass generated per gram of MCM-41 fits well in the curves of Figure 11a,b. For these experiments, the polymers formed have a narrower MWD than those obtained with $(4\text{-}CH_3OC_6H_4)_2CHCl$ or $(C_6H_5)_3CCl$ as the internal surface initiators, because the proton initiation occurs only inside the channel. The lowest cationic reactivity for guest polymerization in MCM-41 shows 2-chlorethyl vinyl ether. Mainly, oligomeric fractions with low molecular weight are obtained for this monomer. Representative results for guest polymerizations of VEs inside MCM-41 are compiled in Table 7.

Comparison of the two methods clearly indicates that an additional initiator is not essential. However, the polymer fraction which remains inside the MCM-41 pores always possesses a lower molecular weight than those of the soluble fractions. It is still not clear which part of the extractable fraction is formed inside the pores, because the critical section in the pore is near the window of the MCM-41. Despite this argument, in ref 44 we have shown that the molecular mass of PEVE can be precisely controlled by MeO as the surface initiator. For producing PVE/MCM-41 hybrids in this

(67) Spange, S.; Eismann, U. *Macromol. Chem. Phys.* **2001**, *202*, 900.

Table 7. Selected Results for Guest Polymerization of VEs inside MCM-41 Compared to the Extractable Fraction, T = 249 K, in 10 mL of Dichloromethane

					M_n [g mol^{-1}]		M_w/M_n	
monomer (batch)	moles [10^4]	initiator	moles [10^4]	MCM-41 [g]	inside MCM-41	extractable	inside MCM-41	extractable
IBVE-4	38	TCl	5.9	0.1	3070	1470	1.6	3.0
IBVE-8	153	TCl	2.0	0.2	8200	23400	3.4	2.3
IBVE-15	19.2			0.11	1750	3700	1.9	2.0
IBVE-17	76			0.21	4700	7200	2.0	2.2
DHF-2	265	MeO	3.2	0.31	4300	15000	2.5	1.7
DHF-4	265			0.3	4100	8000	2.5	1.6
EVE−6	313	MeO	5.2	0.31	4300	6400	1.8	2.2
CHVE-3	17.7	MeO	7.56	0.09	2100	3400	1.7	1.4
CHVE-7	141.2	MeO	1.5	0.17	6270	10500	2.0	1.3
CHVE-11	19.2			0.12	2300	6500	1.7	3.0

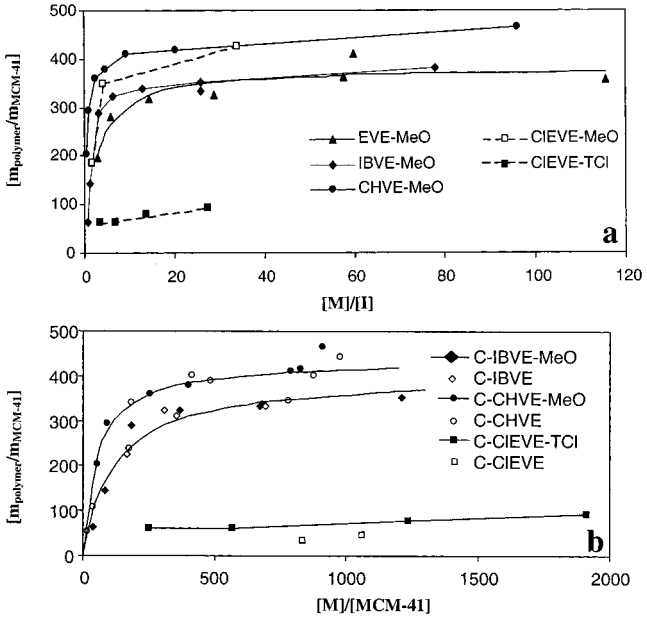

Figure 11. (a) Polymer generated inside MCM-41 as a function of the initial monomer/initiator ratio. (b) Polymer generated within MCM-41 as a function of the initial monomer/MCM-41 ratio. The filled points correspond to MCM-41 with additional an initiator and the hollow points to MCM-41 without an additional internal initiator.

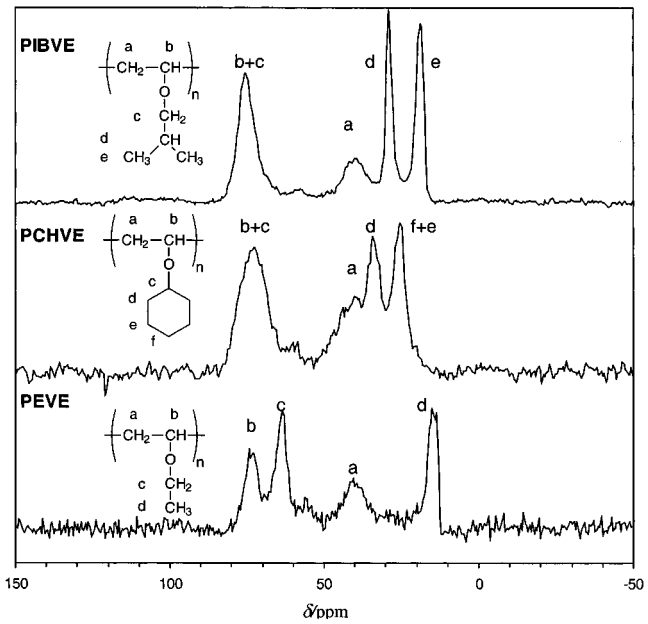

Figure 12. Representative solid-state CP-MAS $^{13}C\{^1H\}$ NMR spectra of PIBVE/MCM-41, PCHVE/MCM-41, and PEVE/MCM-41 hybrid materials. The polymers have been obtained by proton initiation within MCM-41 at 273 K in dichloromethane. The assignment of signals of the carbon atoms to the structure is shown in the inset.

work, we have also used the bare MCM-41 materials without additional initiator.

The PVE/MCM-41 hybrid materials obtained by means of initiation with the bare MCM-41 contain well-defined polymers without structural defects as evidenced by solid-state CP-MAS $^{13}C\{^1H\}$ NMR spectroscopy (Figure 12).

The solid-state CP-MAS $^{13}C\{^1H\}$ NMR spectrum of the PCHVE/MCM-41 hybrid material shows no significant signal at about δ = 10 ppm indicating methyl headgroups. This is a further indication that proton-transfer reactions to the monomer inside the channel are suppressed even at 249 K.

The molecular mass of the polymer fraction inside the channel can be controlled in the range from M_n = 1000 to about 6000 g mol^{-1} (see Table 7). For the EVE polymerization, a good relationship between the molecular mass and the initial monomer/initiator (I) ratio [M]/[MeO] has been established.[44] For the other monomers, the theoretical plot [M]/[I] is satisfactory.

In contrast to the properties of the PVE/HY zeolite materials, the PVE/MCM-41 hybrids are as thermally stable as the pure PVEs because the hybrid materials could be well dried in vacuo and reproducibly measured.

The BET surface area and pore size distribution of the former MCM-41 and resulting PVE/MCM-41 hybrid materials could be determined (Figures 13 and 14).

The pore volume of the PVE/MCM-41 hybrid materials decreases continuously with increasing polymer loading in all investigated samples. The pore radius distribution in the hybrid material becomes correspondingly wider, as can be seen, for example, in the case of MCM-41/PEVE hybrids (Figure 13). PEVE/MCM-41 pores with a smaller radius (r = 1.1−1.8 nm) can be observed alongside pores of unloaded MCM-41 regions (r = 1.82 nm).

For the PNVC/MCM-41 hybrid materials, only a decrease of the whole BET pore volume is observed (Figure 15) with increasing polymer content without narrowing of the pores (Figure 14). The pore diameter of the former material is not decreased. Accordingly, PNVC penetrates only in the window section of the pores. Then it polymerizes rapidly, and the pores become plugged. The rigid PNVC fills this section of the pores completely because PNVC is restricted in its thermal motion because of its larger glass transition temperature compared to PVE.[44,67]

Altogether, these results clearly show that the pores of the MCM-41 are filled with the polymers. The

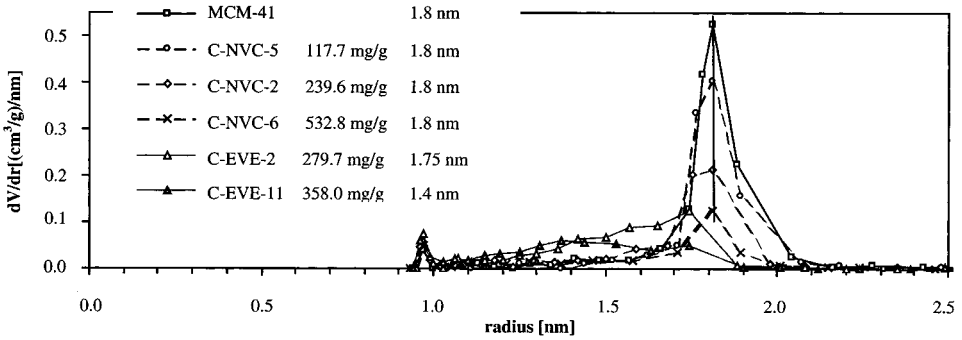

Figure 13. Adsorption of nitrogen per volume [d*V*] as a function of the pore radius [d*r*] for MCM-41, PNVC/MCM-41, and PEVE/MCM-41 hybrid materials with different loadings of polymer. The maximum peak value of each batch is given.

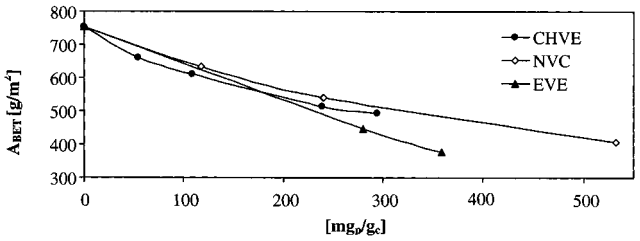

Figure 14. Decrease of the BET surface area for PNVC/MCM-41, PEVE/MCM-41, and PCHVE/MCM-41 with increasing polymer content inside the pores.

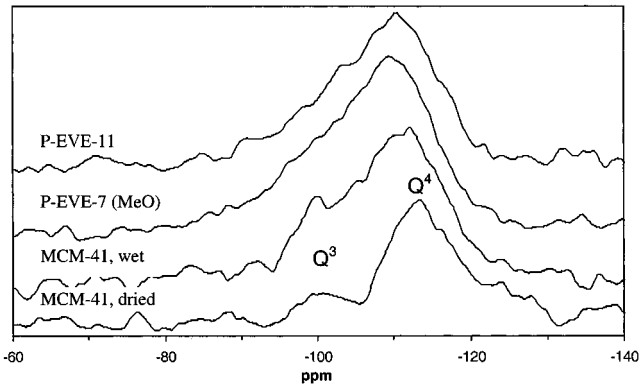

Figure 15. Solid-state MAS ^{29}Si NMR spectra of MCM-41 (dried at 673 K), MCM-41 (nondried, wet), PEVE/MCM-41 hybrid material (proton initiation), and PEVE/MCM-41 (MeO initiation).

polymers are strongly bound to the internal surface of the MCM-41 wall, because they cannot be extracted with solvents suitable for dissolution of PVE or PNVC. On the other hand, PVEs inside MCM-41 show a high mobility as suggested by broad-band dielectric spectroscopic measurements.[44] Therefore, the glass transition temperature of PVE chains under the condition of constricted geometry is significantly decreased (for further details, see ref 44).

The strong bonding of the polymer to the MCM-41 wall can be attributed either to a covalent Si−O−C bond which can be formed by the reaction of the growing cationically active chain with the silanol groups, which nucleophilically trapping the chain end,[46] or to strong adsorption of the polymer on the MCM-41 wall.[67]

The Si−O−C bond can be easily identified by solid-state CP-MAS ^{13}C{^{1}H} NMR spectroscopy.[68a,b] The ^{13}C NMR signal for the relevant carbon atom is expected at about $\delta = 58 \pm 2$ ppm. In Figure 12 CP-MAS ^{13}C-{^{1}H} NMR spectra of PVE/MCM-41 hybrid materials measured, a weak signal in this section is observed. In

Chart 5. Reaction of Acetaldehyde Diethyl Acetal with MCM-41 and Assignment of the NMR Signal to Surface Groups NMR Signals Found[a]

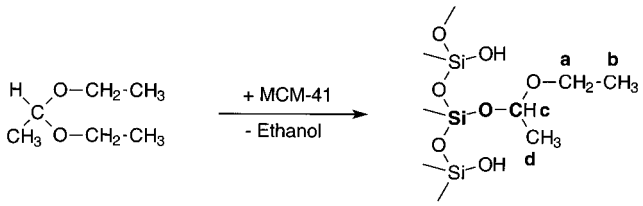

[a] ^{1}H MAS: δ (ppm) = 0.5−1.6 (6H, H^b − H^d), 3.0-4.0 (3H, H^a + H^c) and protons of the residual silanol groups at δ (ppm) = 1.7−3.2. CP-MAS ^{13}C{^{1}H}: δ (ppm) = 63 (C^{c}or C^d), 59 (C^{a}or C^c), 21 (C^d), and 15 (C^b). ^{29}Si MAS: δ (ppm): −110 (Q^4) and −100 (Q^3).

addition, solid-state NMR investigations (^{13}C and ^{29}Si) have so far not given any unambiguous indication as to whether the PVE formed is actually covalently bonded to the inner MCM-41 wall by an Si−O−CHR^{1}OR bond. It is very difficult to differentiate between the ^{13}C NMR signal of the C atom of the Si−O−C bond and that of the end group of the PVE.[68c]

Acetals or ketals react readily with silanol groups forming Si−O−CHR^{1}OR bonds,[69] which is very likely, especially because AAD reacts smoothly with MCM-41 with loss of ethanol (Chart 5).

In the solid-state CP-MAS ^{13}C{^{1}H} NMR spectrum of the product of the reaction between $CH_3CH(OC_2H_5)_2$ and MCM-41, two signals at $\delta = 58.2$ and 58.6 ppm are clearly detectable. They relate to the expected Si−O−C bond and the ether bond of the acetal.[68] An assignment of the two bonds is difficult. However, the reaction of $CH_3CH(OC_2H_5)_2$ with MCM-41 also occurs rapidly at room temperature and, therefore, evidently supports the formation of Si−O−C bonds during the host−guest polymerization of the VEs. As long as water or acidic and basic impurities are excluded, this bond remains stable. This prevents extraction of the polymer by organic solvents. The strong bonding of the PVE to the internal MCM-41 wall is supported by DRIFT spectroscopy (Table 8) and solid-state ^{29}Si NMR spectroscopy (Figure 15).

Table 8 shows the shifts of the $-CH_2-$ vibration of three different PVE chains $[-CH_2CH(OR)-]_n$ inside the

(68) (a) Hoebbel, D.; Nacken, M.; Schmidt, H. *J. Sol−Gel Sci. Technol.* **1998**, *12*, 169. (b) Wies, C.; Meise-Gresch, K.; Müller-Warmuth, W.; Beier, W.; Göktas, A. A.; Frischat, G. H. *Ber. Bunsen-Ges. Phys. Chem.* **1988**, *92*, 689. (c) Spektrenkatalog: In *The Aldrich Library of ^{13}C and ^{1}H FT NMR Spectra*, 1st ed.; Pouchert, C. J., Behneke, J., Eds.; 1993.

(69) Guidotti, B. R.; Herzog, E.; Bangerter, F.; Caseri, W. R.; Suter, U. W. *J. Colloid Interface Sci.* **1997**, *191*, 209.

Table 8. Influence of the Host Matrix of MCM-41 on the CH_2 Vibration of the Guest Polymer Compared to Those of the Bulk (Melt)

	ν [cm^{-1}]		
polymer sample	guest polymer	bulk polymer	difference, $\Delta\nu$ [cm^{-1}]
PEVE	2977.9	2973.6	4.3
	2935.9	2931.2	4.7
	2881.2	2873.4	7.8
PIBVE	2961.5	2954.6	6.9
	2878.7	2872.9	5.8
PCHVE	2936.0	2931.0	5.0
	2861.4	2856.6	4.8

Chart 6. Proposed Adsorption of a PVE Segment on the Internal Silanol Groups of MCM-41

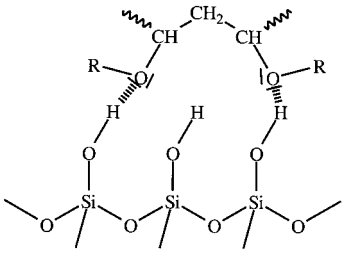

MCM-41 compared to those of the bulk polymers. The $-CH_2-$ vibration of the polymer inside MCM-41 shifts to higher energy compared to that of the bulk polymer. This is a clear indication that the polymer is adsorbed on the internal MCM-41 surface. It is assumed that the oxygen atoms of the absorbed PVE chain interact with the silanol groups (Chart 6). As a consequence, the energy required for inducing the $-CH_2-$ vibration must be larger.

The results of ^{29}Si NMR spectroscopy of the PVE/MCM-41 hybrid materials do not allow a detailed interpretation concerning the bonding of the polymer to the MCM-41 material (see Figure 15), because the spectrum in the section of the Q^3 (O_3Si-OH) and Q^4 (O_3Si-O-) signals of the silica framework is poorly resolved. The ^{29}Si NMR spectrum of the hybrid material only shows a wide Q^4 signal at $\delta = 110$ ppm and no clear Q^3 signal, compared to the unloaded MCM-41 (dried and wet sample) where the Q^3 signal clearly appears.

These results of the ^{29}Si NMR spectra are in line with the previous interpretations. However, they gave no additional information concerning the formation of Si−O−C bonds or the nature of bonding of the polymer to the MCM-41 skeleton.

Morphological Studies. Because heterogeneously induced polymerization in the pores of siliceous materials can be supports for immobilized catalysts (i.e., propylene polymerization initiated by immobilized transition-metal catalysts), the destruction of the siliceous support during the polymerization process is desired. However, this effect is detrimental to the production of nanostructural hybrid materials via host−guest polymerizations.

To prove that the guest polymerizations applied have no negative effect on the morphology of the skeleton of the HY zeolite and MCM-41, transmission electron micrographs of the bare inorganic materials and of the polymer/inorganic hybrids are shown in Figure 16.

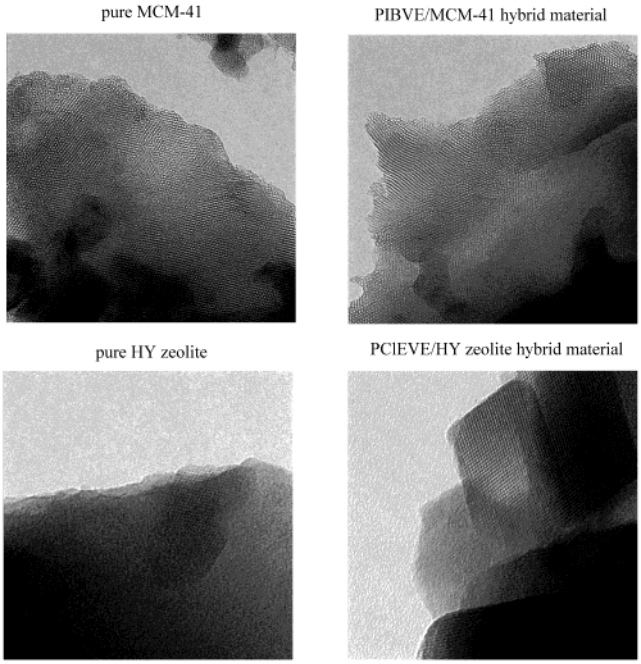

Figure 16. Transmission electron micrographs of the pure porous materials and the resulting inorganic/organic host−guest materials after the polymerization procedure. Note that the morphology of the inorganic host has not been changed.

From the pictures in Figure 16, it is clear that the morphology of the pores of the inorganic materials is not destroyed by the polymers. The channels of the MCM-41 material can be clearly shown in the right picture (left side). They have a length of about 100−150 nm. Note that the polymers have no contrast and cannot be detected by this method.

Conclusion

PVE/HY zeolite and PVE/MCM-41 hybrid materials with adjustable polymer content and molecular weight of the loaded polymer fraction can be synthesized by cationic host−guest polymerization of VE monomers within HY zeolite or MCM-41 materials. For the procedure, the inorganic materials are used in the form of particle powders in a slurry of a solvent suitable for cationic polymerization. The polymer chains in MCM-41 have properties identical with those of the pure and bulk polymers, whereas in the HY zeolite, the original PVE chains are not stable because of the acid-induced ether cleavage caused by the HY skeleton. However, by this method the fabrication of colored PVE/HY zeolite hybrids which are suitable as precursor materials for carbon/HY zeolite composites is possible.

Acknowledgment. This work was supported by the Deutsche Forschungsgemeinschaft within the framework of the program "Nanoporous Host−Guest Systems". We also thank Prof. Dr. M. Antonietti, MPI of Colloids and Interfaces, for the support of the morphological studies, Prof. Holze, TU Chemnitz, for support of the DRIFT studies, and the Fonds der Chemischen Industrie for financial support.

CM011028S